STOKES/ANTI-STOKES RAMAN MICROPROBE ANALYSIS OF LASER-HEATED SILICON MICROSTRUCTURES ON SILICON DIOXIDE

GREGORY D. PAZIONIS, HUA TANG, LEI GE AND IRVING P. HERMAN
Columbia University, Department of Applied Physics, New York, NY 10027

ABSTRACT

Temperatures of laser-heated silicon microstructures on fused silica were determined by Stokes/anti-Stokes scattering using the 4880Å and 5145Å argon-ion laser lines, either separately or together to heat and probe the structure. Phonon shifts and broadening gave consistent measurements of temperature. Evaluation of temperatures from the ratio of Stokes/anti-Stokes intensities was shown to be sensitive to the details of scattering, collection, and detection.

INTRODUCTION

One important class of direct laser-writing reactions involves laser absorption in a micron-sized region of a substrate which induces a similarly localized modification of the surface. In such pyrolytic reactions, the laser absorption induces several important physical changes near the surface, most notably increasing the temperature locally and causing strain formation. In turn, these changes may be modified during "writing" on the substrate because of evolving optical and thermal properties. To understand direct laser writing properly, these physical changes must be characterized theoretically and be monitored experimentally.(1) This paper addresses the physical conditions encountered in direct laser writing studies involving silicon. Experiments are conducted and analyzed in which either one or two lasers are focused on silicon microstructures on SiO_2 (fused silica) to heat the structure and to monitor the physical properties by Stokes/anti-Stokes Raman microprobe methods. The microprobe techniques used here are useful for general in-situ diagnostics of laser and non-laser surface processing in microelectronics.

EXPERIMENTAL SECTION

The silicon microstructures were prepared by depositing a 0.6μm thick polysilicon film on a fused silica substrate by CVD; this film was then patterned by photolithography. For the experiments reported here, disk microstructures with a ~4.4μm diameter are used. In single-beam experiments either the 4880Å or 5145Å line from a cw argon-ion laser is directed into a laser microscope assembly (1) and focused at the center of the disk to a spot size ~ 0.5μm (half-width at 1/e points in laser intensity). Backscattered Raman radiation is collected, dispersed by a spectrometer and detected by a diode array. In two-beam experiments the multi-line output from the argon-ion laser is dispersed by a prism, all wavelengths other than 4880Å and 5145Å are blocked, and the two beams are then recombined by a second prism. The focused beam spot sizes and the precision of two-beam alignment are determined by laterally translating the disk relative to the laser focus, while measuring the laser power transmitted through the microstructure/substrate.

The Raman spectra of such simultaneously heated and probed disks were investigated in one- and two-laser configurations for various laser powers. Figure 1 depicts two such two-laser spectra for 2mW or 8mW laser power at each 4880Å and 5145Å. Note that the 4880Å Stokes and 5145Å anti-Stokes peaks are within a few Å of each other. They were measured simultaneously by the diode array with the spectrometer centered near 5010Å, while the 4880Å anti-Stokes and 5145Å Stokes were each measured individually with the spectrometer tuned near 4759Å and 5286Å, respectively.

ANALYSIS

The spectral differential cross-section for local Stokes scattering from ω_ℓ to $\omega_s = \omega_\ell - \omega_p$ is (2,3):

$$\frac{d^2\sigma_{s,\ell}}{d\Omega d\omega_s} = A\,\frac{\omega_\ell \omega_s{}^3 v}{\omega_p}\left(\frac{\eta_s}{\eta_\ell}\right)\left|\chi_s(\omega_\ell,-\omega_p,T)\right|^2 [n(\omega_p)+1]\,g(\omega_s) \tag{1}$$

and the photon scattering rate is:

$$\frac{d^2R_{s,\ell}}{d\Omega d\omega_s} = \frac{I_\ell}{\hbar\omega_\ell}\,\frac{d^2\sigma_{s,\ell}}{d\Omega d\omega_s} \tag{2}$$

A is a constant; ω is the frequency; v, the local scattering volume; η, the index of refraction; χ, the polarization-averaged Raman susceptibility; n, the phonon occupation number; and $g(\omega_s)$ is the lineshape, where the subscripts ℓ, s and p refer to the laser, Stokes radiation, and phonon, respectively. The lineshape is given by:

$$g(\omega_s) = \frac{\Gamma_p(T)/2\pi}{[\omega_s - (\omega_\ell - \omega_p(T))]^2 + [\Gamma_p(T)/2]^2} \tag{3}$$

where ω_p and Γ_p are the optical phonon frequency and linewidth, respectively.

In Raman probing of a disk radius r_d and thickness d, the measured scattering rate is:

$$\frac{d^2R_{s,\ell}}{d\Omega d\omega_s} = \int_0^d \int_0^{r_d} \frac{A'\omega_s{}^3}{\eta_\ell \eta_s \omega_p}\,[t(r,z)I_\ell(r,z)]\,|\chi_s(\omega_\ell,-\omega_p,T)|^2$$

$$\times\ [n(\omega_p)+1]\ g(\omega_s)\ 2\pi r dr dz \tag{4}$$

where $I_\ell(r,z)$ is the local laser intensity:

$$I_\ell(r,z) = (1 - \bar{R}_\ell(r,z)) I_\ell{}^0(r,z)\, e^{-\int_0^z \alpha_\ell(T(r,z))dz} \tag{5}$$

with $\bar{R}$ the reflectivity, $I_\ell{}^0$ the incident laser intensity, α the absorption coefficient, and $t(r,z)$ the trapping factor for the Stokes radiation:

$$t(r,z) = (1 - \bar{R}_s(r,z))\, e^{-\int_0^z \alpha_s(T(r,z))dz} \tag{6}$$

When the temperature profile is non-uniform ($T = T(r,z)$) Eq.(4) must be used because α, ω_p, Γ_p, χ_s and $n(\omega_p)$ are strongly temperature dependent. For uniform and nearly-uniform temperature profiles, Eq. (4) reduces to:

$$\frac{d^2R_{s,\ell}}{d\Omega d\omega_s} = \frac{A''\omega_s{}^3}{\eta_\ell \eta_s \omega_p} \left[\frac{(1-\bar{R}_\ell)(1-\bar{R}_s)}{(\alpha_\ell + \alpha_s)} \left\{ 1-e^{-(\alpha_\ell + \alpha_s)d} \right\} I_\ell{}^0 \right]$$
$$\times \left| \chi_s(\omega_\ell, -\omega_p, T) \right|^2 [n(\omega_p) + 1]\, g(\omega_s) \tag{7}$$

In laser heating of Si disks on SiO_2 the temperature profile in the disk is nearly uniform, since the thermal conductivity of Si is much larger than that of SiO_2. This near uniformity of the disk temperature is demonstrated below, justifying the use of Eq. (7) here and making the Si/SiO_2 system relatively easy to analyze. Analogous expressions exist for anti-Stokes scattering for a laser at frequency $\omega_{\ell'}$ to $\omega_{as} = \omega_{\ell'} + \omega_p$, with $n + 1$ replaced by n and the subscript "s" replaced by "as."

In analysis of Stokes and anti-Stokes scattering Eq. (4) (or Eq. (7)) gives the spectral profiles, while the Stokes/anti-Stokes ratio is given by the appropriate ratio of the integrated spectra of Eq. (4). For nearly-uniform temperature profiles, this ratio is:

$$F_{s/as} = \frac{\dfrac{dR_{s,\ell}}{d\Omega}}{\dfrac{dR_{as,\ell'}}{d\Omega}} = f_{s/as} \frac{I_\ell{}^0}{I_{\ell'}{}^0}\, e^{+\frac{\hbar\omega_p(T)}{kT}} \tag{8}$$

where

$$f_{s/as} = \frac{C_s}{C_{as}} \frac{\eta_{\ell'} \eta_{as}}{\eta_\ell \eta_s} \frac{(1-\bar{R}_\ell)\,(1-\bar{R}_s)}{(1-\bar{R}_{\ell'})(1-\bar{R}_{as})} \left(\frac{\omega_s}{\omega_{as}}\right)^3 \left(\frac{\alpha_{\ell'}+\alpha_{as}}{\alpha_\ell+\alpha_s}\right) \left(\frac{1-e^{-(\alpha_\ell+\alpha_s)\, d}}{1-e^{-(\alpha_{\ell'}+\alpha_{as})d}}\right)$$
$$\times \frac{|\chi_s(\omega_\ell, -\omega_p, T)|^2}{|\chi_{as}(\omega_{\ell'}, +\omega_p, T)|^2} \tag{9}$$

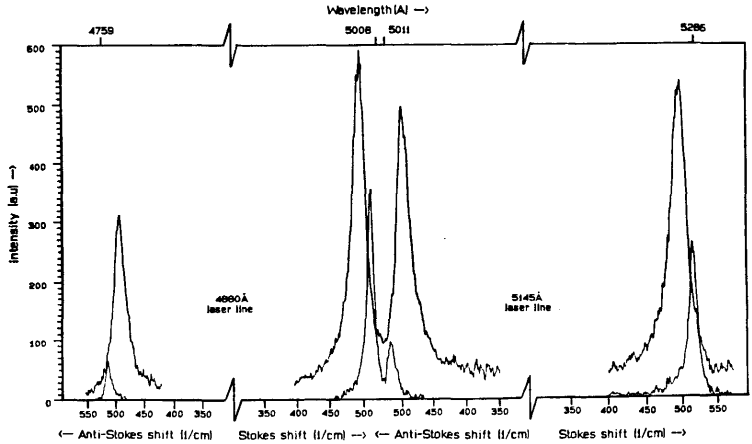

Figure 1. Raman spectra vs. wavelength and frequency shift for two-beam Si/SiO_2 experiments. Of the four pairs of peaks, the relatively larger ones were obtained with 8.0mW 4880Å + 8.1mW 5145Å, while the relatively smaller peaks were obtained with 2.2mW 4880Å + 2.1mW 5145Å. From left to right, the peaks are the 4880Å anti-Stokes (~4759Å), 4880Å Stokes (~5008Å), 5145Å anti-Stokes (~5011Å), and the 5145Å Stokes (~5286Å), respectively.

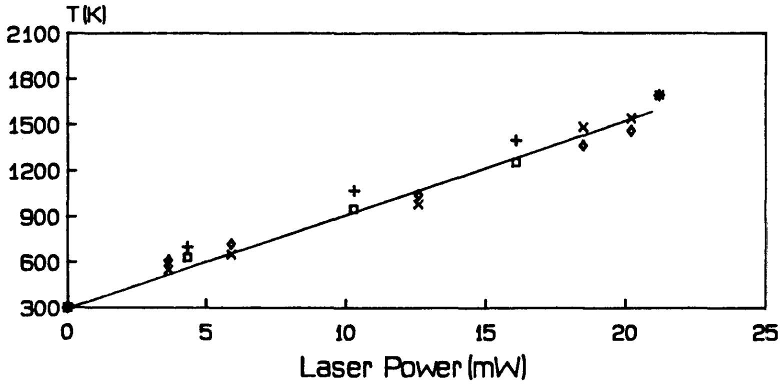

Figure 2. The temperature derived from the Raman microprobe analysis versus total laser power. One-beam experiments (4880Å) were used to obtain T from ω_p (◊) or Γ_p (x), and two-beam experiments (4880Å/5145Å equal power) were also employed to determine T from ω_p(□) or Γ_p(+). * denotes the observed melting point.

C is the spectral collection/detection sensitivity. With this, then f may be calculated from known spectroscopic parameters.(2,3,4)

The phonon frequency of the Si disk varies with temperature as for bulk c-Si,(5) with a small correction for stress:

$$\omega_p(T) = \omega_p^{c\text{-}Si}(T) + \Delta\omega_p^{stress}(T) \tag{10}$$

Using a model of stress induced in laser-heated microstructures(6):

$$\Delta\omega_p^{stress}(T) = 2.0\times10^{-3}(T - 811)\mathrm{cm}^{-1}. \tag{11}$$

where T is in Kelvin. Similarly, the phonon linewidth is

$$\Gamma_p(T) = \Gamma_p^{c\text{-}Si}(T) + \Gamma^{stress} + \Gamma(T,\delta T) \quad , \tag{12}$$

where the first term is that for c-Si,(5) the second term is due to stress inhomogeneities ($\simeq$2.8 cm^{-1}), and the third term is the extra linewidth due to the inhomogeneous temperature in the probed region. When Eq. (4) is used this last term is zero. This term is needed when Eq. (7) is used and therefore when the temperature variation δT is small:

$$\Gamma(T,\delta T) \sim \left| \frac{d\omega_p^{c\text{-}Si}(T)}{dT} \delta T \right| \quad . \tag{13}$$

For T~1400K, $d\omega_p^{c\text{-}Si}/dT \sim -0.037\mathrm{cm}^{-1}/K$. If the temperature gradient is large, as for Si disks on sapphire, Eq. (4) must be used. For Si/SiO_2 this $\Gamma(T,\delta T)$ correction is small and Eq. (7) (with Eq. (13)) is a satisfactory approximation.

The temperature profiles of the laser-heated microstructures were calculated using finite difference analysis of the steady-state heat flow equation,(6) similar to that used by Piglmayer et al.(7) in their study of laser-heated disks. Raman spectral profiles were simulated using these temperature distributions in Eq. (4), though for the case of Si/SiO_2 under discussion direct use of Eq. (7) is fine. Both the laser heating and Raman profile calculations permitted analysis of either single- or double-beam studies. For an incident laser power of 15mW the temperature calculation (6) predicts that the temperature of the disk decreases by only ~10% from the peak value at (r=0,z=0) to the minimum disk T (at $r=r_d=2.2\mu m$, z=d=0.6μm), and decreases by only ~4% from the peak value to the edges of the laser probed region (r~0.5μm, $z=(\alpha_\ell+\alpha_s)^{-1} \sim 0.2\mu m$ at high T), thus justifying the use of Equation (7).

The Raman shifts and linewidths were measured from experiments such as the two depicted in Figure 1. As expected, consistent values for ω_p and Γ_p were obtained for either the Stokes or anti-Stokes peak using either laser wavelength. Peak disk temperatures were determined using Eq. (7) with either $\omega_p(T)$ [Eqs. 10,11] or $\Gamma_p(T)$ [Eqs. 12,13] and are plotted vs. total laser power in Figure 2 for the cases of one-laser (4880Å) and two-laser (4880Å/5145Å equal power) heating and probing. Temperatures derived using either ω_p or Γ_p are consistent with each other and with the observed laser power required to melt these polysilicon disks on fused silica (~21mW at the laser focus), though temperatures derived from Γ_p were often slightly higher than those derived from ω_p. Ignoring the stress correction [Eq. (11)] to ω_p in Eq. (10), would lead to a temperature overestimate of ~50K at T=1500K.

Care must be exercised in evaluating T from the scattered intensities using Eq. (8). If f were (improperly) assumed to be 1.0, the temperatures derived from the 4880Å Stokes/5145Å anti-Stokes spectra would be abnormally high (>>melting). Oven heated c-Si (T = 600K) was examined by the two-beam technique and analyzed using Eqs.(8) and (9) with known values of α.(4) Each of the four pairs of Stokes/anti-Stokes spectra gave the same correct value of T with $|\chi_s(\omega_\ell + \omega_p, -\omega_p, T)/\chi_s(\omega_\ell, -\omega_p, T)|^2 = 1.09$. This is consistent with the 1.1 value of the square of this Raman susceptibility ratio for (sub-band gap) green light, as calculated in Ref. 2. However, use of these parameters in Eqs. (8) and (9) did not give consistent temperatures for the Si/SiO_2 Stokes/anti-Stokes measurements. Equivalently, the measured values of f for two-beam analysis of c-Si and Si/SiO_2 differed somewhat for each of the four Stokes/anti-Stokes pairs. Experimental studies of Stokes/anti-Stokes scattering in oven heated Si/SiO_2 are underway to examine this further.

Using 0.013 W/cm-K for the thermal conductivity of fused silica at room temperature, the thermal calculation predicts a peak temperature of ~1300K for a total laser power of 20mW. This is somewhat lower than the value (~1500K) derived from the Raman spectra, probably because of the too high value of the fused silica thermal conductivity employed here.

Experimental work on Raman analysis of temperature and stress effects during laser writing is continuing.

ACKNOWLEDGMENTS

This work is supported by the Office of Naval Research. One of the authors (GDP) has also been supported by an IBM Postdoctoral Fellowship.

REFERENCES

1. F. Magnotta and I. P. Herman, Appl. Phys. Lett. 48, 195 (1986).

2. G. E. Jellison, Jr., D. H. Lowndes, and R. F. Wood, Phys. Rev. B28, 3272 (1983).

3. A. Compaan and H. J. Trodahl, Phys. Rev. B29, 793 (1984).

4. G. E. Jellison, Jr. and F. A. Modine, Appl. Phys. Lett. 41, 180 (1982).

5. M. Balkanski, R. G. Wallis, and E. Haro, Phys. Rev. B28, 1928 (1983).

6. G. D. Pazionis, H. Tang, and I. P. Herman (in preparation).

7. K. Piglmayer, J. Doppelbauer, and D. Bauerle, in Laser-Controlled Chemical Processing of Surfaces--MRS Vol. 29, edited by A. W. Johnson, D. J. Ehrlich, and H. R. Schlossberg (North Holland, New York, 1984), p.47.